Acta Cryst E CRYSTALLOGRAPHIC COMMUNICATIONS

ISSN 2056-9890

Synthesis, crystal structure and thermal reactivity of diaquadithiocyanatobis(pyridine-4-carbonitrile)-cobalt(II)

Christian Näther*

Institut für Anorganische Chemie, Universität Kiel, Max-Eyth.-Str. 2, 24118 Kiel, Germany. *Correspondence e-mail: cnaether@ac.uni-kiel.de

Received 4 May 2026
Accepted 17 July 2026

Edited by F. Di Salvo, University of Buenos Aires, Argentina

Keywords: synthesis; crystal structure; cobalt thiocyanate; aqua complex; 4-cyanopyridine; hydrogen bonding; thermal properties.

CCDC reference: 2574033

Supporting information: this article has supporting information at journals.iucr.org/e

The title compound, $[Co(NCS)_2(C_6H_4N_2)_2(H_2O)_2]$, is isotypic to its Ni analog and to one of the two modifications of $Mn(NCS)_2$(4-cyanopyridine)$(H_2O)_2$ reported recently [Näther (2026). *Acta Cryst.* E**82**, 441–445 and Wellm *et al.* (2020). *Cryst. Growth Des.* **20**, 3374–3385]. Its asymmetric unit is built up of one cobalt cation that occupies a center of inversion, one thiocyanate anion, one neutral 4-cyanopyridine coligand and one water molecule that are located in general positions. The metal cations are sixfold coordinated by two terminally N-bonding thiocyanate anions, two water molecules and two 4-cyanopyridine coligands within a slightly distorted octahedral geometry. The discrete complexes are linked by intermolecular O—H···S hydrogen bonding into layers that condense into a three-dimensional network *via* weak C—H···N interactions. Powder X-ray diffraction (PXRD) proves that a pure sample has been obtained. Thermogravimetric measurements reveal that the title compound decomposes in different steps, in which compounds with the composition $Co(NCS)_2$(4-cyanopyridine)$_2$ and $Co(NCS)_2$(4-cyanopyridine) are formed as intermediates, which are not isotypic to the corresponding Mn compounds already reported in the literature [Wellm *et al.* (2020). *Cryst. Growth Des.* **20**, 3374–3385].

1. Chemical context

The synthesis of new coordination compounds with desired physical properties is still a major goal in coordination chemistry (Ferrando-Soria *et al.*, 2017; Yue & Gao, 2019). In most cases, such compounds are prepared in solution but there are alternatives such as, for example, molecular milling (Braga *et al.*, 2005, 2006; James *et al.*, 2012; Do & Friščić, 2017; Stolar *et al.*, 2017) or reactions in melts (Müller-Buschbaum, 2005; Höller & Müller-Buschbaum, 2008; Zurawski *et al.*, 2012), which represent typical solid-state synthesis methods. Many years ago, we established a further very simple method that can be used for the synthesis of coordination compounds with condensed coordination networks. In the beginning, this method was used to prepare transition-metal halide and pseudohalide coordination compounds (Näther *et al.*, 2002) but it was later expanded to coordination compounds based on transition-metal thio- and selenocyanates (Näther & Greve, 2003; Wriedt & Näther, 2010; Wöhlert *et al.*, 2012). Following this route, simple precursor compounds such as discrete complexes with terminally thio- or selenocyanate anions are heated, which frequently leads to a stepwise removal of the neutral coligands and the formation of coligand-deficient intermediate phases in which the metal cations are linked by bridging anionic ligands. These intermediate compounds are of interest because they can show interesting

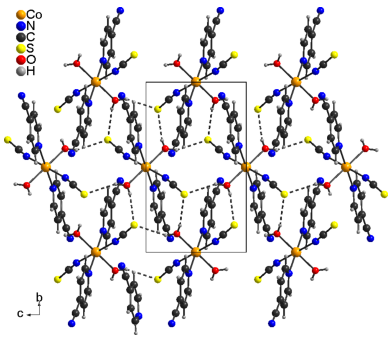

magnetic properties that are mediated by the bridging anionic ligands (Wöhlert *et al.*, 2013; Neumann *et al.*, 2018). In this context, compounds based on $Co(NCS)_2$ or $Co(NCSe)_2$ are of special interest, because they can show 1D and 3D magnetic ordering (Lescouëzec *et al.*, 2005; Mautner *et al.*, 2018; Rams *et al.*, 2020).

In the course of our work, we investigated the influence of the coligand, which mostly consists of pyridine derivatives, because in this case the thermal treatment of the precursor leads to compounds with 1D or 2D thio- or selenocyanate networks. Within this project we became interested in 4-cyanopyridine as coligand, which can in principle also act as bridging ligand and for which some compounds were already reported (see *Database survey*). With $Mn(NCS)_2$ we obtained a large number of compounds with different ratios between $Mn(NCS)_2$ and 4-cyanopyridine (Wellm *et al.*, 2020), including the discrete complex $Mn(NCS)_2$(4-cyanopyridine)$_4$ (refcode OJEDOZ; Wellm *et al.*, 2020) as well as two different modifications of $Mn(NCS)_2$(4-cyanopyridine)$_2(H_2O)_2$ (OJEFAN and OJEFAN01; Wellm *et al.*, 2020), one of which is isotypic to the title compound and to $Ni(NCS)_2$(4-cyanopyridine)$_2$-$(H_2O)_2$ reported recently (Näther, 2026). Two further aqua complexes of same composition but with additional 4-cyanopyridine as solvate ligand were also obtained (OJEFER and OJEFUH; Wellm *et al.*, 2020). If the aqua complex is heated, a transformation is observed into $Mn(NCS)_2$(4-cyanopyridine)$_2$ (OJEFIV; Wellm *et al.*, 2020), which transforms into $Mn(NCS)_2$(4-cyanopyridine) (OJEDUF and OJEDUF01; Wellm *et al.*, 2020) upon further heating. For the latter compound, two different isomers were obtained.

To investigate whether a corresponding aqua complex with $Co(NCS)_2$ is available and if it will show a similar reactivity to that with $Mn(NCS)_2$, we reacted $Co(NCS)_2$ with 4-cyanopyridine using similar conditions as for the synthesis of $Mn(NCS)_2$(4-cyanopyridine)$_2(H_2O)_2$. The crystals obtained by this procedure were characterized by single-crystal X-ray diffraction.

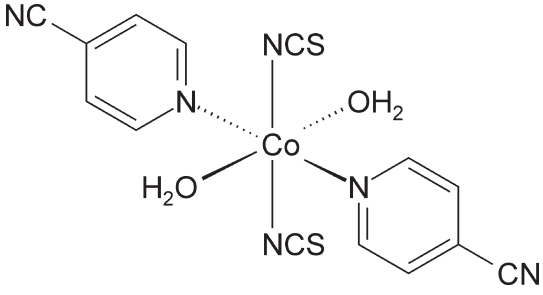

2. Structural commentary

The title compound $Co(NCS)_2(C_6H_4N_2)_2(H_2O)_2$ ($C_6H_4N_2$ = 4-cyanopyridine) is isotypic to $Ni(NCS)_2$(4-cyanopyridine)$_2$-$(H_2O)_2$ (Näther, 2026) reported recently and to one of the two modifications of $Mn(NCS)_2$(4-cyanopyridine)$_2(H_2O)_2$ (OJEFAN; Wellm *et al.*, 2020).

The asymmetric unit consists of one Co cation that is located on a center of inversion, as well as one thiocyanate anion, one 4-cyanopyridine ligand and one water molecule that are located in general positions. The metal cations are sixfold coordinated by two terminally N-bonding thiocyanate anions, two water molecules and two 4-cyanopyridine ligands that coordinate with the pyridine N atom to the metal center (Fig. 1). This arrangement leads to the formation of discrete complexes, which show a slightly distorted octahedral coordination (see supporting information).

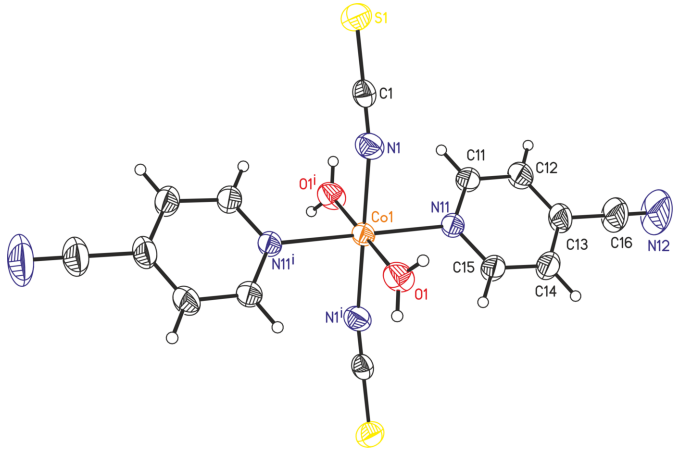

Figure 1
Crystal structure of the title compound with labeling and displacement ellipsoids drawn at the 50% probability level. Symmetry code: (i) $-x+1$, $-y+1$, $-z$.

3. Supramolecular features

In the crystal structure of the title compound, the discrete complexes are connected *via* intermolecular O—H···S hydrogen bonding between the thiocyanate S atom and the H

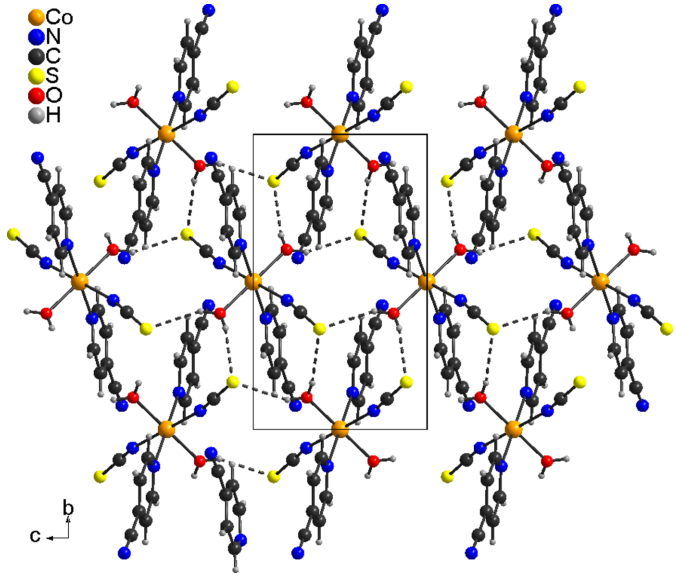

Figure 2
Crystal structure of the title compound in a view along the crystallographic *a*-axis direction with intermolecular O—H···S hydrogen bonding shown as dashed lines.

Table 1
Hydrogen-bond geometry (Å, °).

D—H···A	D—H	H···A	D···A	D—H···A
O1—H1A···S1^{i}	0.82 (2)	2.50 (2)	3.2272 (17)	150 (3)
O1—H1B···S1^{ii}	0.81 (2)	2.53 (2)	3.3227 (16)	168 (3)
C15—H15···N12^{iii}	0.93	2.45	3.144 (3)	132

Symmetry codes: (i) $-x+1, -y+1, -z+1$; (ii) $-x+1, y-\frac{1}{2}, -z+\frac{1}{2}$; (iii) $-x+2, y-\frac{1}{2}, -z+\frac{1}{2}$.

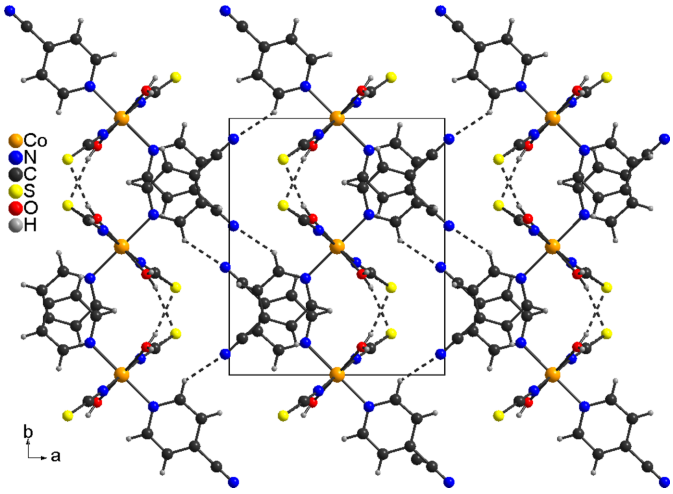

Figure 3
Crystal structure of the title compound in a view along the crystallographic *c*-axis direction with intermolecular O—H···S and C—H···N hydrogen bonding shown as dashed lines.

atoms of the water molecules. Each water molecule is involved in two hydrogen bonds to S atoms of neighboring complexes and each S atom acts as acceptor for two hydrogen bonds to two different water molecules (Fig. 2). This arrangement leads to the formation of ten-membered hydrogen-bonded rings involving three symmetry-related complexes. These rings condense into layers that are parallel to the *bc* plane (Fig. 2). The O–H···S angles are close to linearity, indicating relatively strong interactions (Table 1).

The layers are linked by pairs of C—H···N interactions between the pyridine N atom of one complex and the cyano N atom of a neighboring complex, forming hydrogen-bonded rings that are located around centers of inversion (Fig. 3). From this interaction, a three-dimensional network is formed (Fig. 3). The C—H···N angle is far from linear, indicating a weak interaction (Table 1).

4. Additional characterization

The experimental powder pattern of crystals of the title compound was compared with that calculated from single-crystal data, proving that a pure crystalline phase had been obtained (Fig. 4). The CN stretching vibration of the thiocyanate anion is observed at 2094 cm^{-1} in the IR spectrum, in agreement with terminal coordinated anionic ligands and the presence of water is obvious from the strong band at 3343 cm^{-1} (Fig. S1).

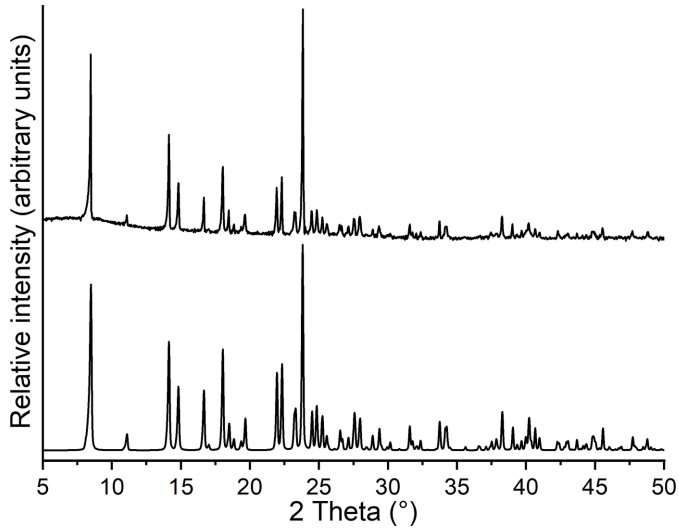

Figure 4
Experimental (top) and calculated (bottom) PXRD patterns for the title compound.

Investigations using thermogravimetry (DTA-TG) reveal that the title compound decomposes in three different reasonably resolved steps (Fig. 5). The first mass loss of 8.6% is in perfect agreement with that calculated for the loss of the two water molecules (8.6%). Upon further heating, two similar steps of 24.7 and 24.5% are observed, which should each correspond to the loss of one 4-cyanopyridine ligand in each step ($\Delta m_{calc.}$: 24.8%). Therefore, one can assume that after the first mass loss a compound with the composition $Co(NCS)_2$(4-cyanopyridine)$_2$ is formed, which decomposes into $Co(NCS)_2$)(4-cyanopyridine) upon further heating. After the third mass loss $Co(NCS)_2$ is formed. It is noted, that similar results are reported for the thermal reactivity of $Mn(NCS)_2$(4-cyanopyridine)$_2$(H_2O)$_2$ (Wellm *et al.*, 2020).

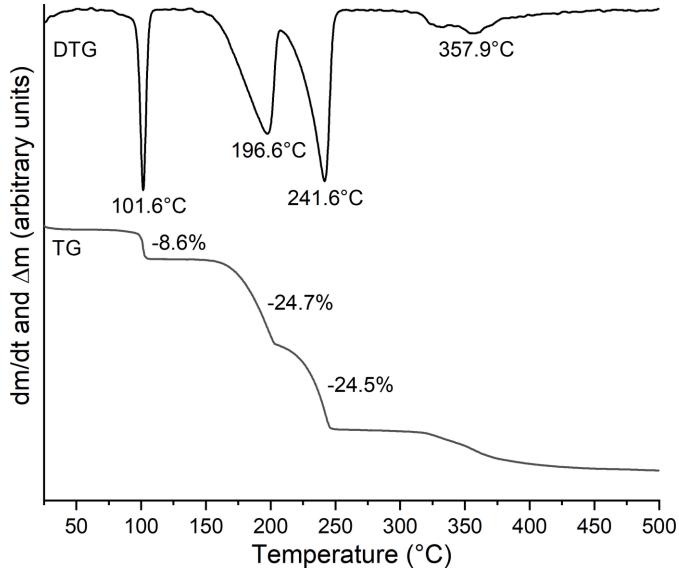

Figure 5
DTG and TG curves for the title compound. The mass loss is given together with the peak temperature (in °C).

To further characterize the intermediate compounds obtained by thermogravimetry, the residues isolated after the first and second mass loss were investigated by powder X-ray diffraction. Comparison of the experimental pattern of the residue obtained after the first step with that calculated for $Mn(NCS)_2$(4-cyanopyridine)$_2$ retrieved from the literature (Wellm *et al.*, 2020) indicates that this crystalline phase is present and that additional reflections are observed, indicating for a further crystalline phase (Fig. S2). However, the overall quality of the pattern is relatively low, indicating that a poorly crystalline powder was obtained. If the powder pattern of the residue obtained after the second mass loss is compared with that calculated for both isomers of $Mn(NCS)_2$(4-cyanopyridine), it is obvious that a completely different and unknown crystalline phase has formed (Fig. S3).

5. Synthesis and crystallization

General:

$Co(NCS)_2$ and 4-cyanopyridine were purchased from Sigma-Aldrich.

Synthesis:

2 mmol (354.2 mg) $Co(NCS)_2$ and 4 mmol (416.4 mg) 4-cyanopyridine were reacted in 3 mL of water. Within 2 d, crystals suitable for crystal structure analysis were obtained.

Experimental details

Powder X-ray diffraction measurements were performed using a Stoe STADI P transmission powder diffractometer with Cu $K\alpha_1$ radiation (λ= 1.540598 Å), equipped with a Johann-type Ge(111) monochromator and a MYTHEN 1K detector from Dectris.

Thermogravimetry measurements were performed in a dynamic nitrogen atmosphere in Al_2O_3 crucibles with a heating rate of 4 °C min^{-1} using a STA-PT 1000 thermobalance from Linseis.

IR spectroscopy was done using an ATI Mattson Genesis Series FTIR Spectrometer, control software: *WINFIRST*, from ATI Mattson in ATR mode.

6. Database survey

A search in the Cambridge Structural Database (CSD Version 5.43, last update January 2026; Groom *et al.*, 2016) using CONQUEST (Bruno *et al.*, 2002) revealed that some compounds with 4-cyanopyridine and transition metal cations are already published. These include discrete complexes with the composition $Ni(NCS)_2$(4-cyanopyridine)$_4$ (UBUBOL; Clegg & Harrington, 2016) and $Mn(NCS)_2$(4-cyanopyridine)$_4$ (OJEDOZ; Wellm *et al.*, 2020) that are not isotypic as well as aqua complexes with the composition $Ni(NCS)_2$(4-cyanopyridine)$_2(H_2O)_2$ (YANHAB; Näther, 2026) and two different modifications of $Mn(NCS)_2$(4-cyanopyridine)$_2(H_2O)_2$ (OJEFAN and OJEFAN01; Wellm *et al.*, 2020) one of which is isotypic to the nickel and the title compounds. Discrete complexes with additional 4-cyanopyridine as solvate are also known, including the isotypic compounds $Fe(NCS)_2$(4-cyanopyridine)$_2(H_2O)_2$·(4-cyanopyridine)$_2$ (KAPQEA; Jochim *et al.*, 2017) and $Mn(NCS)_2$(4-cyanopyridine)$_2(H_2O)_2$·(4-cyanopyridine)$_2$ (OJEFUH; Wellm *et al.*, 2020) as well as $Mn(NCS)_2$(4-cyanopyridine)$_2(H_2O)_2$·(4-cyanopyridine)$_4$ (OJEFER; Wellm *et al.*, 2020). Compounds with 4-cyanopyridine and bridging thiocyanate anions are also reported. They include $Cd(NCS)_2$(4-cyanopyridine)$_2$ in which the metal cations are linked into chains (WUCLUB; Chen *et al.*, 2002) and $Cd(NCS)_2$(4-cyanopyridine) (WUCMAI; Chen *et al.*, 2002) in which the 4-cyanopyridine ligand acts as a bridging ligand. Finally, $Cu(NCS)_2$(4-cyanopyridine)$_2$ is also found, which exhibits a structure similar to that of the corresponding Mn compound (ABOVOF; Handy *et al.*, 2017).

7. Refinement

Crystal data, data collection and structure refinement details are summarized in Table 2. The C—H hydrogen atoms were positioned with idealized geometry and were refined with $U_{iso}(H) = 1.2U_{eq}(C)$ using a riding model. The O—H hydrogen atoms were located in difference maps and were refined isotropic with $U_{iso}(H) = 1.5U_{eq}(O)$ using restraints.

Acknowledgements

This work was supported by the State of Schleswig-Holstein.

Table 2
Experimental details.

Crystal data	
Chemical formula	$[Co(NCS)_2(C_6H_4N_2)_2(H_2O)_2]$
M_r	419.35
Crystal system, space group	Monoclinic, $P2_1/c$
Temperature (K)	298
a, b, c (Å)	10.7397 (5), 12.3497 (8), 7.4967 (4)
β (°)	104.596 (4)
V (Å^3)	962.21 (9)
Z	2
Radiation type	Mo $K\alpha$
μ (mm^{-1})	1.13
Crystal size (mm)	0.20 × 0.16 × 0.12
Data collection	
Diffractometer	Stoe IPDS2
Absorption correction	Numerical (*X-SHAPE* and *X-RED* 32; Stoe, 2008)
T_{min}, T_{max}	0.765, 0.910
No. of measured, independent and observed [$I > 2\sigma(I)$] reflections	15445, 2301, 2058
R_{int}	0.031
(sin $\theta/\lambda)_{max}$ (Å^{-1})	0.660
Refinement	
$R[F^2 > 2\sigma(F^2)]$, $wR(F^2)$, S	0.034, 0.085, 1.10
No. of reflections	2301
No. of parameters	121
No. of restraints	3
H-atom treatment	H atoms treated by a mixture of independent and constrained refinement
$\Delta\rho_{max}$, $\Delta\rho_{min}$ (e Å^{-3})	0.40, −0.29

Computer programs: *X-AREA* (Stoe, 2008), *SHELXT* (Sheldrick, 2015*a*), *SHELXL* (Sheldrick, 2015*b*), *DIAMOND* (Brandenburg, 1999), *XP* in *SHELXTL-PC* (Sheldrick, 2008) and *publCIF* (Westrip, 2010).

References

Braga, D., Curzi, M., Grepioni, F. & Polito, M. (2005). *Chem. Commun.* pp. 2915–2917.

Braga, D., Giaffreda, S. L., Grepioni, F., Pettersen, A., Maini, L., Curzi, M. & Polito, M. (2006). *Dalton Trans.* pp. 1249–1263.

Brandenburg, K. (1999). *DIAMOND*. Crystal Impact GbR, Bonn, Germany.

Bruno, I. J., Cole, J. C., Edgington, P. R., Kessler, M., Macrae, C. F., McCabe, P., Pearson, J. & Taylor, R. (2002). *Acta Cryst.* B**58**, 389–397.

Chen, W., Liu, F. & You, X. (2002). *Bull. Chem. Soc. Jpn* **75**, 1559–1560.

Clegg, W. & Harrington, R. W. (2016). *CSD Communication* (refcode UBUBOL). CCDC, Cambridge, England.

Do, J. L. & Friščić, T. (2017). *ACS Cent. Sci.* **3**, 13–19.

Ferrando-Soria, J., Vallejo, J., Castellano, M., Martínez-Lillo, J., Pardo, E., Cano, J., Castro, I., Lloret, F., Ruiz-García, R. & Julve, M. (2017). *Coord. Chem. Rev.* **339**, 17–103.

Groom, C. R., Bruno, I. J., Lightfoot, M. P. & Ward, S. C. (2016). *Acta Cryst.* B**72**, 171–179.

Handy, J. V., Ayala, G. & Pike, R. D. (2017). *Inorg. Chim. Acta* **456**, 64–75.

Höller, C. J. & Müller-Buschbaum, K. (2008). *Inorg. Chem.* **47**, 10141–10149.

James, S. L., Adams, C. J., Bolm, C., Braga, D., Collier, P., Friščić, T., Grepioni, F., Harris, K. D. M., Hyett, G., Jones, W., Krebs, A., Mack, J., Maini, L., Orpen, A. G., Parkin, I. P., Shearouse, W. C., Steed, J. W. & Waddell, D. (2012). *Chem. Soc. Rev.* **41**, 413–447.

Jochim, A., Jess, I. & Näther, C. (2017). *Acta Cryst.* E**73**, 463–466.

Lescouëzec, R., Toma, L. M., Vaissermann, J., Verdaguer, M., Delgado, F. S., Ruiz-Pérez, C., Lloret, F. & Julve, M. (2005). *Coord. Chem. Rev.* **249**, 2691–2729.

Mautner, F. E., Traber, M., Fischer, R. C., Torvisco, A., Reichmann, K., Speed, S., Vicente, R. & Massoud, S. S. (2018). *Polyhedron* **154**, 436–442.

Müller-Buschbaum, K. (2005). *Z. Anorg. Allg. Chem.* **631**, 811–828.

Näther, C. (2026). *Acta Cryst.* E**82**, 441–445.

Näther, C. & Greve, J. (2003). *J. Solid State Chem.* **176**, 259–265.

Näther, C., Greve, J. & Jess, I. (2002). *Solid State Sci.* **4**, 813–820.

Neumann, T., Ceglarska, M., Germann, L. S., Rams, M., Dinnebier, R. E., Suckert, S., Jess, I. & Näther, C. (2018). *Inorg. Chem.* **57**, 3305–3314.

Rams, M., Jochim, A., Böhme, M., Lohmiller, T., Ceglarska, M., Rams, M. M., Schnegg, A., Plass, W. & Näther, C. (2020). *Chem. Eur. J.* **26**, 2837–2851.

Sheldrick, G. M. (2008). *Acta Cryst.* A**64**, 112–122.

Sheldrick, G. M. (2015*a*). *Acta Cryst.* A**71**, 3–8.

Sheldrick, G. M. (2015*b*). *Acta Cryst.* C**71**, 3–8.

Stoe (2008). *X-AREA*, *X-RED32* and *X-SHAPE*. Stoe & Cie, Darmstadt, Germany.

Stolar, T., Batzdorf, L., Lukin, S., Žilić, D., Motillo, C., Friščić, T., Emmerling, F., Halasz, I. & Užarević, K. (2017). *Inorg. Chem.* **56**, 6599–6608.

Wellm, C., Neumann, T., Gallo, G., Dziubyna, A. M., Rams, M., Dinnebier, R. E. & Näther, C. (2020). *Cryst. Growth Des.* **20**, 3374–3385.

Westrip, S. P. (2010). *J. Appl. Cryst.* **43**, 920–925.

Wöhlert, S., Ruschewitz, U. & Näther, C. (2012). *Cryst. Growth Des.* **12**, 2715–2718.

Wöhlert, S., Wriedt, M., Fic, T., Tomkowicz, Z., Haase, W. & Näther, C. (2013). *Inorg. Chem.* **52**, 1061–1068.

Wriedt, M. & Näther, C. (2010). *Chem. Commun.* **46**, 4707–4709.

Yue, G. & Gao, E. Q. (2019). *Coord. Chem. Rev.* **382**, 1–31.

Zurawski, A., Rybak, J. C., Meyer, L. V., Matthes, P. R., Stepanenko, V., Dannenbauer, N., Würthner, F. & Müller-Buschbaum, K. (2012). *Dalton Trans.* **41**, 4067–4078.

supporting information

Acta Cryst. (2026). E**82**, 952-956 [https://doi.org/10.1107/S2056989026007371]

Synthesis, crystal structure and thermal reactivity of diaquadithiocyanatobis-(pyridine-4-carbonitrile)cobalt(II)

Christian Näther

Computing details

Diaquadithiocyanatobis(pyridine-4-carbonitrile)cobalt(II)

Crystal data

$[Co(NCS)_2(C_6H_4N_2)_2(H_2O)_2]$
M_r = 419.35
Monoclinic, $P2_1/c$
a = 10.7397 (5) Å
b = 12.3497 (8) Å
c = 7.4967 (4) Å
β = 104.596 (4)°
V = 962.21 (9) Å^3
Z = 2
$F(000)$ = 426
D_x = 1.447 Mg m^{-3}
Mo $K\alpha$ radiation, λ = 0.71073 Å
Cell parameters from 8000 reflections
θ = 10.0–25.0°
μ = 1.13 mm^{-1}
T = 298 K
Block, light blue
0.20 × 0.16 × 0.12 mm

Data collection

Stoe IPDS-2 diffractometer
ω scans
Absorption correction: numerical (X-Shape and X-Red 32; Stoe, 2008)
T_{min} = 0.765, T_{max} = 0.910
15445 measured reflections
2301 independent reflections
2058 reflections with $I > 2\sigma(I)$
R_{int} = 0.031
θ_{max} = 28.0°, θ_{min} = 2.6°
h = −12→14
k = −16→16
l = −9→9

Refinement

Refinement on F^2
Least-squares matrix: full
$R[F^2 > 2\sigma(F^2)]$ = 0.034
$wR(F^2)$ = 0.085
S = 1.10
2301 reflections
121 parameters
3 restraints
Hydrogen site location: mixed
H atoms treated by a mixture of independent and constrained refinement
$w = 1/[\sigma^2(F_o^2) + (0.0386P)^2 + 0.2457P]$ where $P = (F_o^2 + 2F_c^2)/3$
$(\Delta/\sigma)_{max} < 0.001$
$\Delta\rho_{max}$ = 0.40 e Å^{-3}
$\Delta\rho_{min}$ = −0.29 e Å^{-3}

Special details

Geometry. All esds (except the esd in the dihedral angle between two l.s. planes) are estimated using the full covariance matrix. The cell esds are taken into account individually in the estimation of esds in distances, angles and torsion angles; correlations between esds in cell parameters are only used when they are defined by crystal symmetry. An approximate (isotropic) treatment of cell esds is used for estimating esds involving l.s. planes.

Fractional atomic coordinates and isotropic or equivalent isotropic displacement parameters (Å²)

	x	*y*	*z*	U_{iso}*/U_{eq}
Co1	0.500000	0.500000	0.000000	0.04781 (12)
N1	0.41307 (18)	0.56286 (14)	0.1939 (3)	0.0650 (4)
C1	0.34588 (18)	0.60302 (14)	0.2716 (3)	0.0517 (4)
S1	0.24962 (5)	0.65987 (5)	0.38157 (8)	0.07134 (17)
O1	0.61498 (16)	0.39204 (12)	0.1917 (2)	0.0700 (4)
H1A	0.636 (3)	0.402 (2)	0.303 (2)	0.105*
H1B	0.656 (3)	0.342 (2)	0.170 (4)	0.105*
N11	0.64730 (14)	0.62443 (11)	0.0722 (2)	0.0541 (4)
N12	1.0191 (3)	0.9194 (3)	0.2427 (7)	0.1738 (18)
C11	0.6192 (2)	0.72943 (15)	0.0807 (3)	0.0632 (5)
H11	0.533302	0.749637	0.059118	0.076*
C12	0.7119 (2)	0.80896 (16)	0.1201 (4)	0.0730 (6)
H12	0.689078	0.881551	0.121478	0.088*
C13	0.8386 (2)	0.77856 (17)	0.1572 (4)	0.0722 (6)
C14	0.8698 (2)	0.67080 (18)	0.1518 (4)	0.0733 (6)
H14	0.955171	0.648522	0.177556	0.088*
C15	0.77105 (18)	0.59709 (16)	0.1071 (3)	0.0643 (5)
H15	0.791685	0.524276	0.101000	0.077*
C16	0.9401 (3)	0.8582 (2)	0.2035 (6)	0.1074 (11)

Atomic displacement parameters (Å²)

	U^{11}	U^{22}	U^{33}	U^{12}	U^{13}	U^{23}
Co1	0.04761 (19)	0.03533 (16)	0.0581 (2)	0.00129 (12)	0.00883 (14)	−0.00217 (13)
N1	0.0719 (11)	0.0523 (9)	0.0745 (11)	−0.0030 (8)	0.0254 (9)	−0.0088 (8)
C1	0.0549 (10)	0.0418 (8)	0.0557 (10)	−0.0082 (7)	0.0088 (8)	−0.0016 (7)
S1	0.0606 (3)	0.0821 (4)	0.0734 (4)	0.0073 (3)	0.0207 (3)	−0.0045 (3)
O1	0.0813 (10)	0.0519 (8)	0.0678 (9)	0.0139 (7)	0.0023 (8)	0.0019 (7)
N11	0.0483 (8)	0.0389 (7)	0.0707 (10)	0.0018 (6)	0.0070 (7)	−0.0040 (7)
N12	0.104 (2)	0.101 (2)	0.295 (5)	−0.0540 (19)	0.009 (3)	−0.033 (3)
C11	0.0528 (10)	0.0414 (9)	0.0910 (15)	0.0045 (8)	0.0097 (10)	−0.0084 (9)
C12	0.0699 (13)	0.0394 (9)	0.1041 (17)	−0.0022 (9)	0.0113 (12)	−0.0120 (10)
C13	0.0641 (12)	0.0533 (11)	0.0932 (16)	−0.0151 (9)	0.0087 (11)	−0.0103 (11)
C14	0.0476 (10)	0.0589 (11)	0.1054 (18)	−0.0009 (9)	0.0045 (11)	−0.0061 (12)
C15	0.0496 (10)	0.0420 (9)	0.0946 (15)	0.0039 (7)	0.0056 (10)	−0.0032 (9)
C16	0.0757 (17)	0.0678 (15)	0.167 (3)	−0.0211 (13)	0.0083 (19)	−0.0175 (18)

Geometric parameters (Å, º)

Co1—N1	2.0667 (18)	N11—C11	1.336 (2)
Co1—N1^{i}	2.0668 (18)	N12—C16	1.118 (3)
Co1—O1	2.1150 (14)	C11—C12	1.376 (3)
Co1—O1^{i}	2.1151 (14)	C11—H11	0.9300
Co1—N11^{i}	2.1738 (15)	C12—C13	1.371 (3)
Co1—N11	2.1738 (15)	C12—H12	0.9300

N1—C1	1.148 (2)	C13—C14	1.375 (3)
C1—S1	1.634 (2)	C13—C16	1.445 (3)
O1—H1A	0.816 (17)	C14—C15	1.373 (3)
O1—H1B	0.805 (17)	C14—H14	0.9300
N11—C15	1.332 (2)	C15—H15	0.9300

N1—Co1—N1^{i}	180.0	C15—N11—C11	117.55 (16)
N1—Co1—O1	92.79 (7)	C15—N11—Co1	119.82 (12)
N1^{i}—Co1—O1	87.21 (7)	C11—N11—Co1	122.62 (13)
N1—Co1—O1^{i}	87.21 (7)	N11—C11—C12	122.90 (19)
N1^{i}—Co1—O1^{i}	92.79 (7)	N11—C11—H11	118.5
O1—Co1—O1^{i}	180.0	C12—C11—H11	118.5
N1—Co1—N11^{i}	90.64 (7)	C13—C12—C11	118.36 (19)
N1^{i}—Co1—N11^{i}	89.36 (7)	C13—C12—H12	120.8
O1—Co1—N11^{i}	89.26 (6)	C11—C12—H12	120.8
O1^{i}—Co1—N11^{i}	90.74 (6)	C12—C13—C14	119.73 (19)
N1—Co1—N11	89.36 (7)	C12—C13—C16	120.8 (2)
N1^{i}—Co1—N11	90.64 (7)	C14—C13—C16	119.4 (2)
O1—Co1—N11	90.74 (6)	C15—C14—C13	118.0 (2)
O1^{i}—Co1—N11	89.26 (6)	C15—C14—H14	121.0
N11^{i}—Co1—N11	180.0	C13—C14—H14	121.0
C1—N1—Co1	166.48 (18)	N11—C15—C14	123.42 (18)
N1—C1—S1	179.7 (2)	N11—C15—H15	118.3
Co1—O1—H1A	124 (2)	C14—C15—H15	118.3
Co1—O1—H1B	127 (2)	N12—C16—C13	178.7 (5)
H1A—O1—H1B	107 (3)		

Symmetry code: (i) −*x*+1, −*y*+1, −*z*.

Hydrogen-bond geometry (Å, º)

D—H···*A*	*D*—H	H···*A*	*D*···*A*	*D*—H···*A*
O1—H1*A*···S1^{ii}	0.82 (2)	2.50 (2)	3.2272 (17)	150 (3)
O1—H1*B*···S1^{iii}	0.81 (2)	2.53 (2)	3.3227 (16)	168 (3)
C15—H15···N12^{iv}	0.93	2.45	3.144 (3)	132

Symmetry codes: (ii) −*x*+1, −*y*+1, −*z*+1; (iii) −*x*+1, *y*−1/2, −*z*+1/2; (iv) −*x*+2, *y*−1/2, −*z*+1/2.